blood®
Regular Article

IMMUNOBIOLOGY AND IMMUNOTHERAPY

Potentiating antibody-dependent killing of cancers with CAR T cells secreting CD47-SIRPα checkpoint blocker

Megan M. Dacek,[1,2,*] Keifer G. Kurtz,[1,2,*] Patrick Wallisch,[1,2] Stephanie A. Pierre,[1,3] Shireen Khayat,[2,4] Christopher M. Bourne,[1,5] Thomas J. Gardner,[1] Kristen C. Vogt,[1,6] Nica Aquino,[7] Anas Younes,[8] and David A. Scheinberg[1,2,8]

[1]Molecular Pharmacology Program, Sloan Kettering Institute, New York, NY; [2]Pharmacology Program and [3]Tri-institutunal MD-PhD Program, Weill Cornell Medicine, New York, NY; [4]Immunology Program, Sloan Kettering Institute, New York, NY; [5]Immunology and Microbial Pathogenesis Program, Weill Cornell Medicine, New York, NY; [6]Tri-Institutional PhD Program in Chemical Biology, Weill Cornell Medicine, Memorial Sloan Kettering Cancer Center, The Rockefeller University, New York, NY; and [7]Antitumor Assessment Core and [8]Department of Medicine, Memorial Sloan Kettering Cancer Center, New York, NY

KEY POINTS

- **"Orexi" CAR T cells in combination with an orthogonally targeted monoclonal antibody are more effective than traditional CAR T cells.**
- **OrexiCAR T cells reversed immunosuppression of tumor microenvironment myeloid cells.**

Chimeric antigen receptor (CAR) T-cell therapy has shown success in the treatment of hematopoietic malignancies; however, relapse remains a significant issue. To overcome this, we engineered "Orexi" CAR T cells to locally secrete a high-affinity CD47 blocker, CV1, at the tumor and treated tumors in combination with an orthogonally targeted monoclonal antibody. Traditional CAR T cells plus the antibody had an additive effect in xenograft models, and this effect was potentiated by CAR T-cell local CV1 secretion. Furthermore, OrexiCAR-secreted CV1 reversed the immunosuppression of myelomonocytoid cells both in vitro and within the tumor microenvironment. Local secretion of the CD47 inhibitor bypasses the CD47 sink found on all cells in the body and may prevent systemic toxicities. This combination of CAR T-cell therapy, local CD47 blockade, and orthogonal antibody may be a combinatorial strategy to overcome the limitations of each monotherapy.

Introduction

Although studies on initial chimeric antigen receptor (CAR) T-cell therapy in B-cell acute leukemia have reported response rates as high as 80% to 90%, a high level of relapse is observed because of multiple tumor escape mechanisms, including the lower expression or complete loss of expression of the CD19 antigen from the surface of the cancer cells.[1-3] In addition, highly immunosuppressive tumor microenvironments (TMEs) pose a significant hurdle and greatly limit the efficacy of CAR T cells and other immunotherapeutics.

CAR T cells can be engineered to deliver additional agents locally to tumor sites after proliferation, which we have broadly termed as "targeted cellular micropharmacies."[4-12] Thus, CAR T cells that can co-opt the endogenous immune system show superior efficacy in preclinical models; local delivery of potent, orthogonally acting agents can be achieved without the systemic toxicities usually observed, thereby enhancing the therapeutic index.[9]

Innate immune cell activation is a hallmark of successful CAR T-cell therapy.[13,14] Cytokines that are derived from the CAR T cells themselves as well as endogenous immune effectors are systemically elevated in patients undergoing treatment.[15,16] Here, we address 2 questions related to improving the efficacy of CAR T cells: we first questioned whether CAR T cells had additive effects with monoclonal antibodies (mAbs) directed toward orthogonal targets on cancer cells, thereby improving potency and possibly overcoming resistance or antigen loss escape. We then questioned whether CAR T cells could be engineered to further potentiate the action of the orthogonal mAb by engineering them to block the CD47-SIRPα signaling axis. This was achieved by creating CAR T cells that secrete a high-affinity SIRPα variant, CV1, capable of shutting down the CD47-SIRPα signaling axis.[17,18] This axis, also known as the "do not eat me" signal, suppresses myeloid and monocytoid cells via binding to SIRPα. We termed the CV1-secreting CAR T cells as "OrexiCAR T cells" because of their potentiation of orexigenic activity, that is, increased macrophage phagocytosis. CD47 is a ubiquitously expressed ligand that is overexpressed

by many different cancers, thereby providing them with an immune escape mechanism.[19-21] Blockade of this pathway with CV1 and other anti-CD47 agents has been shown to improve macrophage phagocytosis, macrophage repolarization toward M1, and macrophage and dendritic cell (DC) cross-priming of $CD8^+$ T cells.[17,18,22-26] Although antibody-based CD47 blockers have caused toxicities, this was not observed with CV1 in vivo.[17] In addition, CV1 was shown to improve a variety of mAbs to treat several different cancers, thereby acting as a broadly applicable adjuvant.[17,18] We therefore chose to engineer CAR T cells to secrete CV1 rather than an anti-CD47 antibody-based protein, given its lack of toxicity, small size, and high affinity.

Here, we demonstrated that CD19 CAR T-cell therapy added to anti-CD20 rituximab therapy via innate immune activation improved the survival of mice bearing human lymphoma xenografts. We show that these effects were markedly improved when using OrexiCAR T cells. Furthermore, local CV1 secretion by OrexiCAR T cells was not absorbed by the peripheral CD47 sink compared with systemically administered CV1. In an immune-competent model, we found that OrexiCAR T cells reprogram the TMEs via DC activation and macrophage priming. This strategy has the potential to enhance CAR T-cell activity against tumors with immunosuppressive microenvironments as well as against heterogeneous tumors and those cancer cells that may have escaped via CAR target antigen loss, without added systemic toxicity.

Methods

Generation of retroviral vectors and producer cell lines; cell culture T-cell isolation

The gene encoding CV1 was cloned into the SFG-γ retroviral vector encoding the well-characterized CD19-targeted and MUC16-targeted second-generation CARs (generously provided by the R Brentjens lab, Memorial Sloan Kettering Cancer Center) to generate 19BBz-CV1-HA (19-Orexi) and 4H11-CV1-HA (4H-Orexi). General methods for cell culture, vector assembly, and transfections are described in supplemental Information, available on the *Blood* website.

T-cell isolation and M2 macrophage generation

Human T cells were isolated from healthy donors after informed consent, in compliance with all relevant ethical regulations and in accordance with IRB 00009377. Peripheral blood mononuclear cells were activated for 2 days with 100 IU/mL interleukin-2 (IL-2) and 50ng/mL anti-CD3. Mouse T cells were isolated from the spleens of naïve mice via mechanical disruption, using a 100 μm cell strainer and were activated overnight with CD3/CD28 Dynabeads (Life Technologies) and 50 IU/mL human IL-2, then transduced as described earlier. Details are given in the supplemental Information.

Macrophages $CD14^+$ peripheral blood mononuclear cells were isolated from healthy donors using MACS Cell Separation (Miltenyi Biotec, #130-050-201). $CD14^+$ cells were differentiated and polarized using a previously described protocol.[27] Only adherent cells were considered properly differentiated. M0 macrophages received only macrophage colony stimulating factor.

Flow cytometry

Detailed methods and gating are described in the supplemental Information.

CD47 blocking assay, CV1 quantitative ELISA, and western blots

Antibody CC2C6 binds to the same epitope of CD47 as SIRPα. After incubation, Raji tumor cells were stained with the anti-human CD47 antibody or the anti-mouse CD47 (rat anti-mouse CD47, PE) and analyzed via flow cytometry. Methods are detailed in the supplemental Information.

Recombinant CV1 tagged with both human influenza virus hemagglutinin (HA) and 6X His epitope tags was produced, and a sandwich enzyme-linked immunosorbent assay (ELISA) was performed to quantify the amount of CV1 using an anti-HA or anti-His and a polyclonal anti-CV1 antibody.

In vivo experiments

All experiments were performed in compliance with an institutional animal care and use committee–approved protocol (96-11-044). Tumor burden was monitored via bioluminescence imaging (BLI), using a Xenogen IVIS Spectrum, and analyzed using Living Image software.

Raji NOD scid γ (NSG) mice received engraftment intraperitoneally (IP) on day 0 with 5×10^5 Raji–green fluorescent protein (Raji-GFP)/Luc tumor cells. For the clodronate experiment, mice were injected with 200 μL of liposomes, either control or clodronate, subsequently on days 1 and 3. For the T-cell preconditioned media (PCM) experiment, CAR T cells were cocultured with Raji tumor cells in vitro for 48 hours at a 1:1 ratio in serum-free media. PCM was collected, cells were spun down, and the supernatant was passed through a 0.45 μM syringe filter.

SCID-beige mice received engraftment intravenously (IV) with 1×10^6 Nalm6 engineered to express human CD20 and GFP/ffLuc or with a 1:2 ratio of Nalm6: Nalm6–CD19-knockout (Nalm6-CD19KO) cells.

C57/BL6 mice were engrafted subcutaneously with 1e6-2e6 B16F10 melanoma cells, engineered to express firefly luciferase using a 1:1 mixture with Matrigel.

Statistical analysis

Data reported are given as the mean ± standard deviation, unless otherwise noted. Statistical significance was indicated accordingly: $*P < .05$, $**P < .01$, and $***P < .001$. Details are given in the supplemental Information.

Results

CAR T cells plus orthogonally targeted mAb show potent antitumor activity in vivo

To investigate the treatment benefit of combining CD19 CAR T cells with a mAb (rituximab) reactive with a different target antigen, CD20, also found on most B-cell neoplasms, we subjected NSG mice to engraftment with Raji Burkitt lymphoma tumor cells ($CD19^+$ or $CD20^+$) and subsequently treated them with CD19 CAR T cells in combination with rituximab or a control mAb (Figure 1A). The combination of CAR T cells and

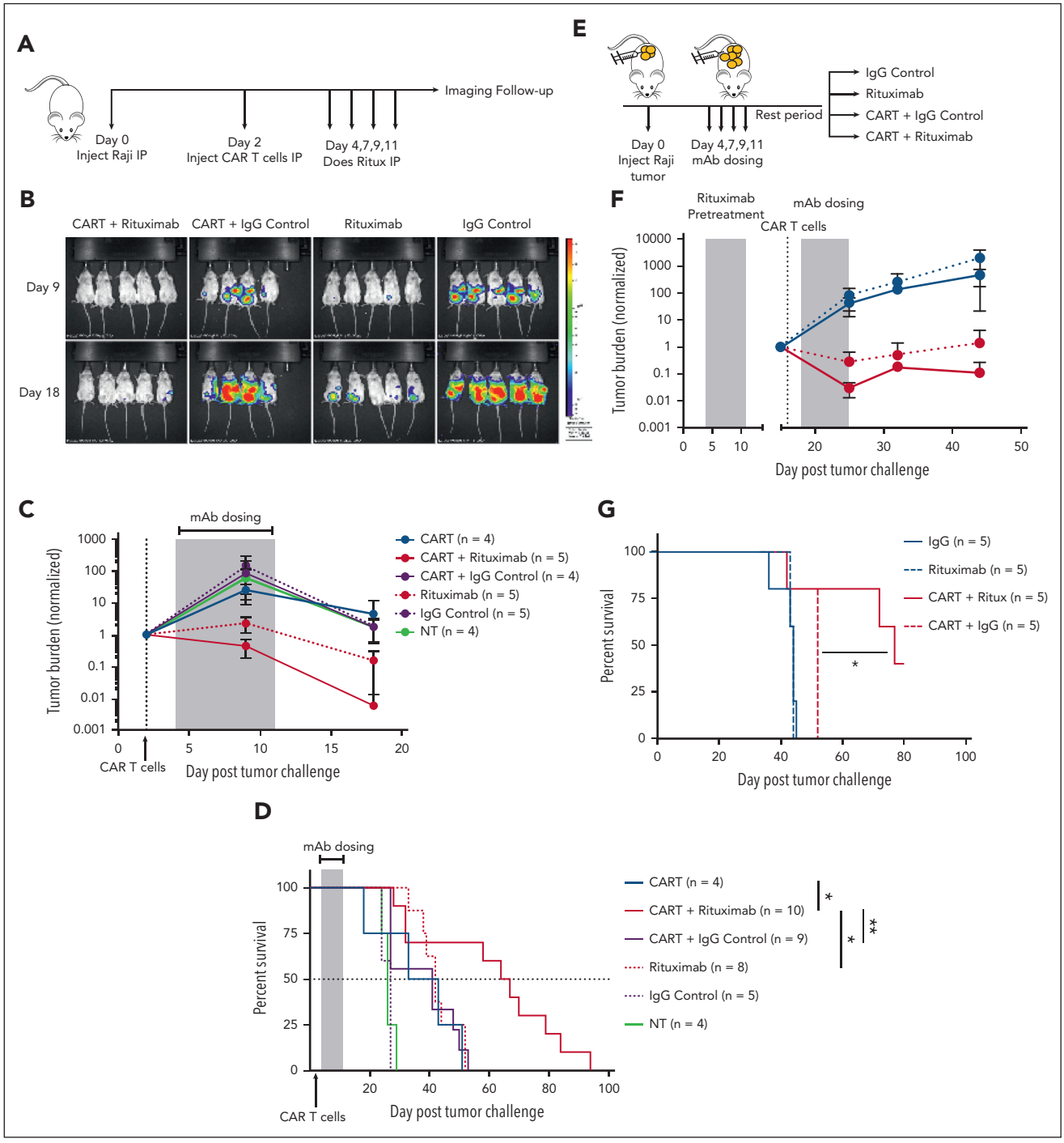

Figure 1. CAR T cells with mAb therapy provides an additive antitumor effect. (A) NSG mice that underwent engraftment IP with Raji-GFP/Luc tumor cells were treated with 5e5 CD19-CAR T cells and 4 total doses of rituximab (100 μg/mouse) on the indicated days. (B) Tumor burden was assessed via BLI and shown for a representative study, and (C) total luminescence was quantified and normalized to pretreatment tumor burden. (D) Survival curves for tumor-bearing mice (2 independent experiments) treated with CD19-targeted CAR T cells and rituximab or a control mAb. (E) NSG mice received engraftment IP with Raji tumors, and all mice received a round of 4 doses (100 μg/mouse) of rituximab. Mice were subsequently divided into the indicated treatment groups. CAR-treated mice were given a dose of 5e5 CAR T cells. (F) Tumor burden was monitored via BLI. See supplemental Figure 2B for the associated survival curve. (G) Overall survival (OS) curves for mice pretreated with rituximab followed by a 10 day rest period. Rituximab-refractory experiment is shown for 1 representative study. See supplemental Figure 2 for replicates. Statistics were performed using a log-rank survival analysis.

rituximab showed a greater reduction in tumor burden (Figure 1B-C) and resulted in a significant additive effect on survival (Figure 1D) as compared with CAR T cells with control mAb or rituximab alone.

To confirm this additive activity in additional tumor models, we subjected SCID-beige mice to engraftment IV with CD19^{+} Nalm6 tumor cells modified to express CD20 (Nalm20-GFP/ffLuc) (supplemental Figure 1A). CAR T cells plus rituximab were

more efficacious than Rituximab or CAR T cells alone in reducing tumor burden (supplemental Figure 1B). Importantly, we saw that the antitumor effect of rituximab was dependent on the binding to its target (CD20), because wild-type (WT; $CD20^{-}$) Nalm6 tumors showed no benefit from the rituximab mAb (supplemental Figure 1D). The precise contributions of antibody-dependent cellular phagocytosis (ADCP), antibody-dependent cellular cytotoxicity (ADCC), complement activation, direct apoptosis, or opsonization are difficult to ascertain in vivo, but the use of the intraperitoneal cavity, which is replete with macrophages, in NSG mice that have no natural killer cells suggests that ADCP may be a dominant mechanism. Additional experiments described further on are dependent on this mechanism.

Because many patients who receive CD19 CAR T-cell therapy have been previously treated with and are refractory to rituximab, we questioned whether CAR T cells could resensitize a rituximab-refractory tumor to rituximab. We repeated the xenograft Raji intraperitoneal model and treated all mice with 1 round of rituximab (Figure 1E). After a rest period to allow relapse, mice were treated with CAR T cells and a second round of rituximab. Mice treated with the second round of rituximab alone, and no CAR T cells, showed no additional antitumor effect compared with mice that were treated with the control mAb, demonstrating these tumors were rituximab-refractory. In contrast, the combination of the CAR T cells with rituximab showed improved tumor control and survival (Figure 1F-G; supplemental Figure 2) as compared with the CAR T cells alone. This suggests that the CAR T cells enhance mAb-mediated killing or vice versa.

Human CAR T cells can be engineered to secrete a CD47 pathway inhibitor

Next, we questioned whether the additive effects of CAR T cells and mAb could be further potentiated by engineering CAR T cells to secrete the truncated SIRPα mimic CV1 (Figure 2A), known to improve mAb therapeutic efficacy. We termed these cells as "OrexiCARs" because they were designed to improve cytotoxicity via enhanced orexigenic activity of ADCP. Primary human T cells transduced with the CD19-OrexiCAR vector showed cell-surface expression of the CAR (Figure 2B) and secretion of functional CV1 (Figure 2C).

CV1 secretion by OrexiCARs increased in response to CAR stimulation by antigen-positive target cells (Figure 2E), supporting the hypothesis that higher intratumoral concentrations of CV1 could be achieved after local T-cell proliferation at the tumor. The use of OrexiCARs may provide 3 advantages compared with the systemic use of CD47 inhibitors: (1) bypassing the large binding sink of CD47 on all cells in the host, (2) reducing systemic toxicities, and (3) overcoming the short plasma half-life of the CV1 agent. Firstly, to investigate the "antigen sink," we injected NSG mice IV with either phosphate-buffered saline, WT, or OrexiCAR T cells. Mice receiving WT CAR T cells were then immediately injected IP with recombinant CV1. Analysis of peripheral blood indicated that although a small amount of CV1 was detectable on peripheral blood cells in OrexiCAR-treated mice, those injected with recombinant CV1 (rCV1) showed 13-fold higher levels bound to blood cells (Figure 2F-G). Secondly, CV1 was previously shown to be nontoxic, compared with Fc-activating anti-CD47 agents,[17] and we confirmed that OrexiCAR T-cell–secreted CV1 was also nontoxic (supplemental Figure 4). Thirdly, because OrexiCAR T cells constitutively express and secrete low levels of CV1, the short half-life of CV1 is negligible, eliminating the need for high and frequent dosing.[28,29] In addition, because of this short half-life, CV1 secreted from OrexiCARs is rapidly cleared.

OrexiCARs demonstrate no functional or activation impairments

To assess the impact CV1 secretion had on CAR T cells themselves, we compared tumor lysis by OrexiCAR T cells with that by conventional CAR T cells. There was no change in cytolytic activity between WT and OrexiCARs (Figure 3A). In addition, there was an increase, although modest, in cytokine secretion by OrexiCARs when compared with that by WT CARs (Figure 3B), but no change in CD4/8 ratios (Figure 3C). These data indicate that CV1 has no detrimental effects and, at most, a small beneficial effect on intrinsic CAR effector functions.

Next, we questioned whether OrexiCARs maintained CV1 secretion after chronic antigen stimulation in vivo. We treated tumor-bearing mice with a suboptimal dose of CAR T cells and analyzed the remaining T cells after 30 days. We found no difference between WT and OrexiCAR T cells in the expression of PD-1, TIM-3, or Lag-3 (Figure 3D). Harvested T cells cultured ex vivo maintained and secreted CV1 at levels sufficient to block CD47 on tumor cells (Figure 3E). The reduction in levels of CD47 found on the cell surface correlated directly with the amount of CV1 elaborated.

Furthermore, a potential downside of the OrexiCAR strategy might be apoptotic T-cell death, as described for several anti-CD47 antibodies.[30-32] Although CV1 bound to and blocked CD47 on the OrexiCARs themselves, it did not induce apoptosis, in contrast to the cytotoxic bivalent anti-CD47 mAb (supplemental Figure 6). This lack of T-cell toxicity is likely because CV1 is a monovalent, noncrosslinking ligand. Taken together, these data demonstrate human T cells can be engineered to coexpress both CAR and CV1 while maintaining T-cell function and simultaneously equipping T cells with a secondary orthogonal mechanism for activating the immune system.

Another potential risk of the OrexiCAR strategy could be the rejection of the CAR T cells themselves via macrophage phagocytosis. Therefore, we cocultured Raji tumor cells, M1 macrophages or M2 macrophages (M2s), and OrexiCARs or WT CAR T cells in vitro. We found that OrexiCARs occupied a higher proportion of the coculture than the WT CAR T cells, indicating that CV1 secretion did not lead to higher levels of CAR T-cell elimination (supplemental Figure 7A). Furthermore, we injected OrexiCARs and WT CAR T cells into NSG mice IP in the absence of tumor and found that OrexiCARs again displayed a slightly elevated, though nonsignificant, proportion of the cell populations retrieved from the intraperitoneal cavity at multiple time points after injection when compared with the WT CARs (supplemental Figure 7B). Therefore, we conclude that secretion of CV1 by OrexiCARs should not lead to their rejection.

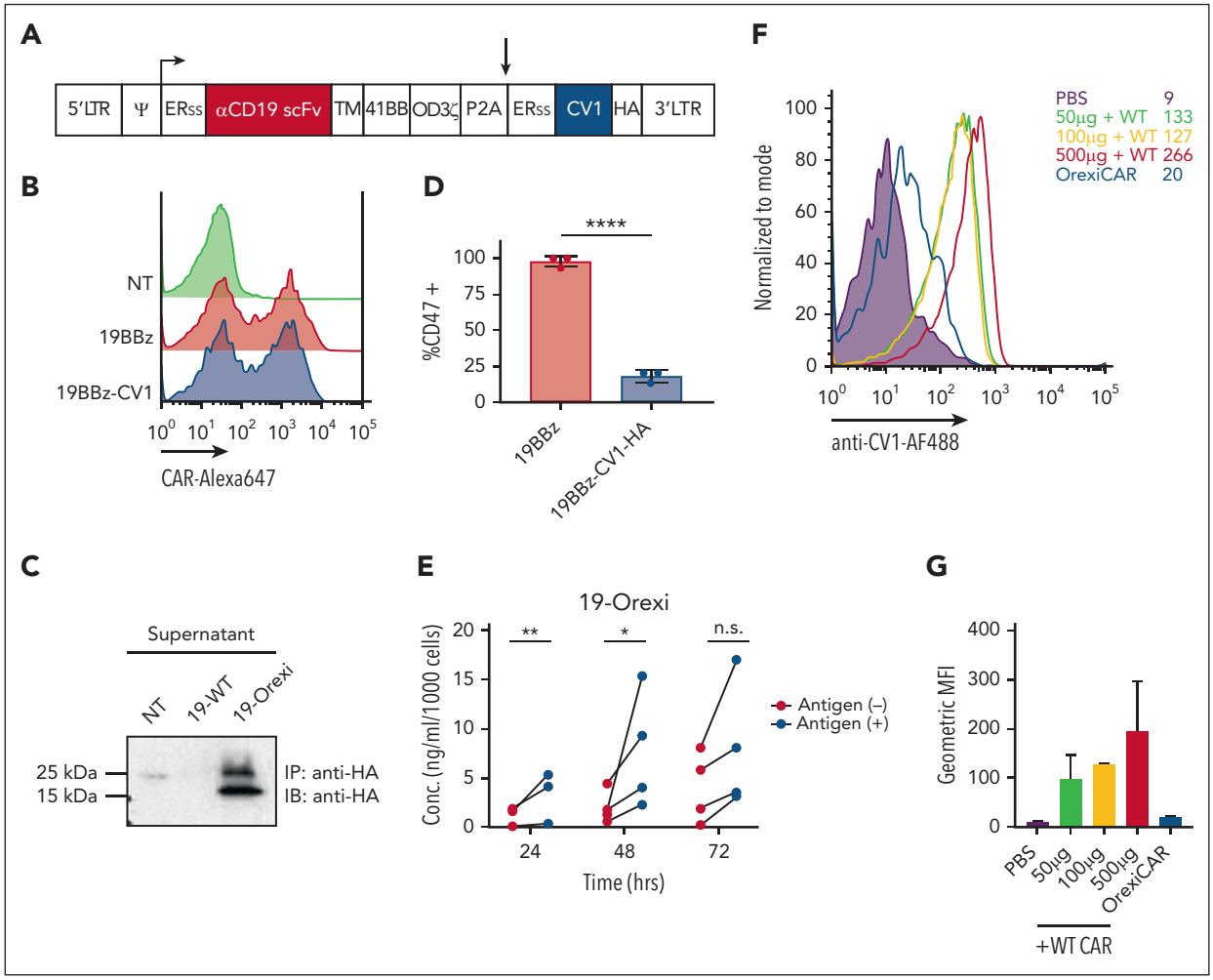

Figure 2. Human CAR T cells can be engineered to express CV1. (A) Vector encoding the CD19 second-generation CAR (19BBz) and CV1 were used to transduce primary human T cells. (B) Transduction efficiency was assessed via flow cytometry, using an anti-idiotype antibody against the anti-CD19 CAR, conjugated to Alexa647 fluorochrome reactive. (C) Supernatant of transduced T cells was subjected to immunoprecipitation and western blot analysis for expression and secretion of CV1. (D) Raji tumor cells were incubated with supernatant from transduced T cells and then subsequently analyzed via flow cytometry for CD47 expression. (E) Secreted CV1 after the coculture of 19BBz Orexi CAR T cells with $CD19^+$ or $CD19^-$ tumor cells, was measured via ELISA (3-4 independent donors). (F) NSG mice were injected IV with either PBS, WT CAR combined with recombinant CV1 at different doses, or OrexiCAR T cells; 1 hour postinjection (p.i.) peripheral blood was collected and analyzed for CV1 occupancy. (G) Quantification of geometric MFI of CV1 staining from panel F. Statistics were performed using student *t* test. ERss, endoplasmic reticulum signal peptide; HA, hemagglutinin epitope tag; MFI, mean fluorescence index; PBS, phosphate-buffered saline; TM, transmembrane domain.

We also compared T-cell function and engraftment in a more clinically relevant subcutaneous tumor model (supplemental Figure 8A). We found no difference between OrexiCARs and WT CARs in the ratio of $CD3^+$ cells to Raji tumor cells in harvested tumors on days 5, 10, and 15 after T-cell injection (supplemental Figure 8B). In addition, there was no difference in the ratio of CAR^+:$CD3^+$ cells at each of these time points (supplemental Figure 8C). We also assessed intratumoral T-cell function by measuring the amount of CD25 on WT and OrexiCARs; we observed an increase, although not significant, of CD25 mean fluorescence index on OrexiCARs at all time points measured, indicating modest enhanced activation status (supplemental Figure 8D). Finally, we investigated the in vivo pharmacokinetics of OrexiCAR secretion in a subcutaneous tumor (Rajis) model in NSG mice (supplemental Figure 8E). Using the previously described CD47 blocking assay, we observed increased intratumoral CV1 concentrations from day 5 (115 ng) to day 10 (321 ng) after T-cell injection and then a decrease at day 15 after T-cell injection (170 ng). The pattern of intratumoral CV1 levels was consistent with the observed activation state of OrexiCARs (supplemental Figure 8D-E). Taken together, these in vitro and in vivo data demonstrated that CV1 does not alter the immune function and pharmacokinetics of OrexiCARs.

OrexiCARs potentiate mAb antitumor activity in vivo

Because relapse with CD19-low or -negative disease is a frequent tumor escape mechanism of CD19-targeted CAR T cells[2], we tested the ability of OrexiCAR T cells to eliminate $CD19^-$ cancer cells using NSG mice engrafted IV with a 1:2 ratio of Nalm6:Nalm6-CD19KO tumor cells, both expressing GFP/Luc (Figure 4A). 9 days after engraftment, OrexiCAR-treated mice had a significantly reduced tumor burden compared with WT-treated mice. Although a single dose of rCV1 in combination with WT CAR T cells also reduced tumor burden at early time points, as expected in this mixed antigen-expressing

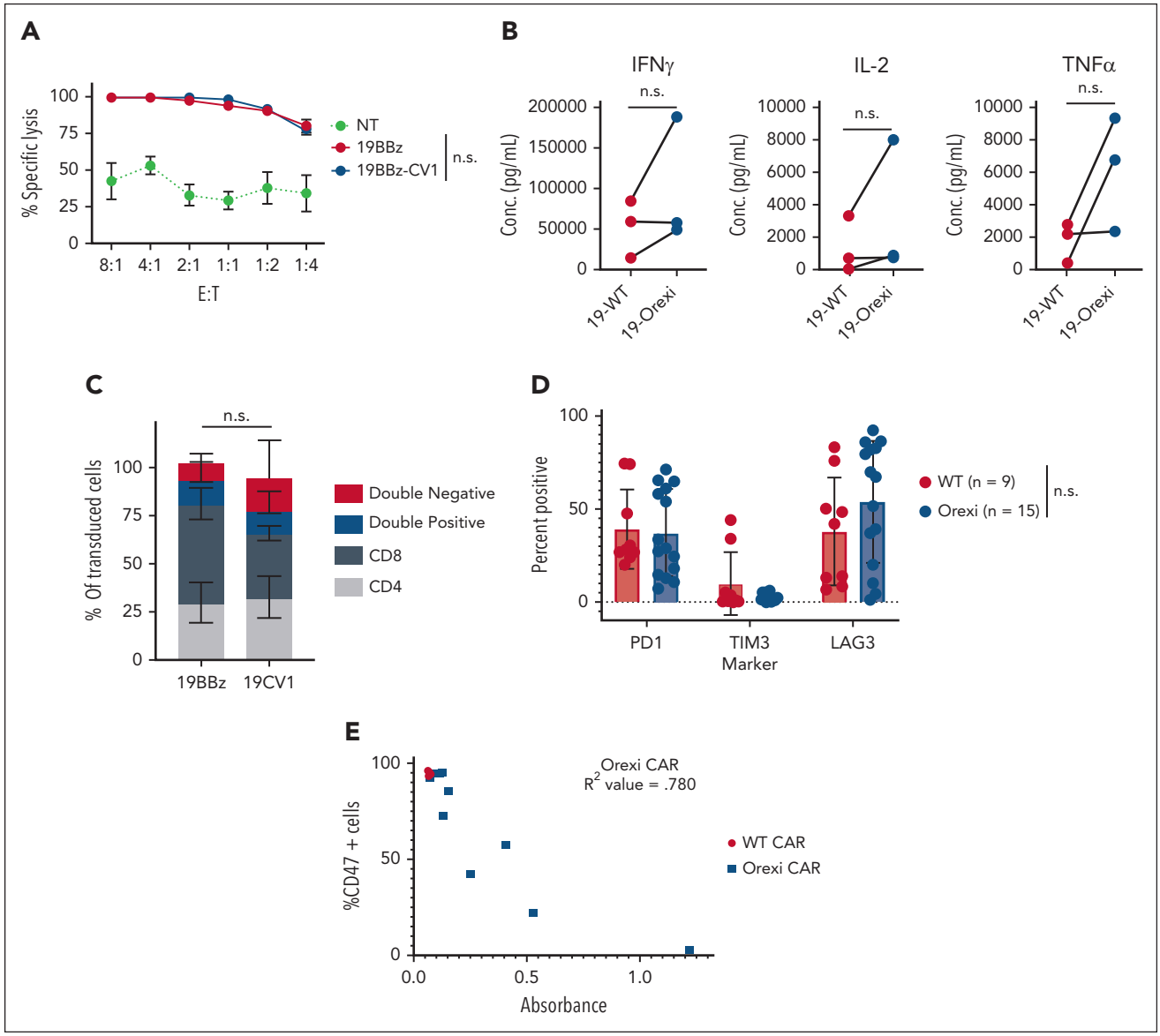

Figure 3. CV1 does not hinder intrinsic CAR effector function. (A) 16 hour tumor lysis by WT and OrexiCAR T cells against CD19$^+$ Raji. Average of 3 donors ± SEM. (B) Cytokine secretion was measured using Luminex after a 24 hour coculture with antigen plus tumor cells. Lines connect matched donors. (C) CD4/8 makeup of transduced cells (CD19$^-$CAR$^+$) was measured via flow cytometry (average of 4 donors). (D) NSG mice that underwent engraftment with Raji tumor cells were treated with WT or OrexiCAR T cells. After 30 days of engraftment, tumors were harvested by intraperitoneal lavage, and infiltrating T cells were analyzed via flow cytometry. (E) Cells isolated from the intraperitoneal cavity were cultured ex vivo and supernatant was analyzed for CV1 secretion, shown as absorbance, via ELISA after 4 days. The same supernatant was used to assess CD47 blocking of Raji tumor cells, shown as the percentage of CD47 cells. R^2 value was determined using a standard linear regression analysis. n.s., not significant; SEM, standard error of mean; TNF, tumor necrosis factor.

model in which two-thirds of the cells were not targets of the CAR, rCV1 plus CAR T cells did not lead to a survival benefit likely because the rapidly growing antigen-negative cells grew out (Figure 4C-D). OrexiCAR T cells provided a small tail of survival. These data show OrexiCAR T cells alone have enhanced antitumor efficacy in vivo against an antigen-low–expressing tumor. However, previous studies indicated that CV1 is significantly more efficacious in conjunction with mAb therapy.[17,18]

Hence, to test whether OrexiCAR T cells could potentiate orthogonal antitumor mAb activity, NSG mice were subjected to engraftment with Raji tumor cells IP and were subsequently treated with WT CAR T cells or OrexiCARs in combination with a control antibody or rituximab (Figure 4E). Rituximab alone provided a minimal antitumor effect. However, there was greatly enhanced tumor control (>10 000× reduction in median BLI) by OrexiCARs in combination with rituximab compared with all other groups (Figure 4F-G). OrexiCARs and WT CAR T cells have the same antitumor efficacy when used as single agents in this model (Figure 4F), suggesting that OrexiCARs further enhanced the activity of rituximab compared with WT CAR T cells. In addition, 80% of the mice treated with OrexiCARs and rituximab had no detectable tumor (Figure 4G) at day 86 after tumor engraftment, as compared with only 20% of the mice treated with WT CAR T cells. This antitumor effect also

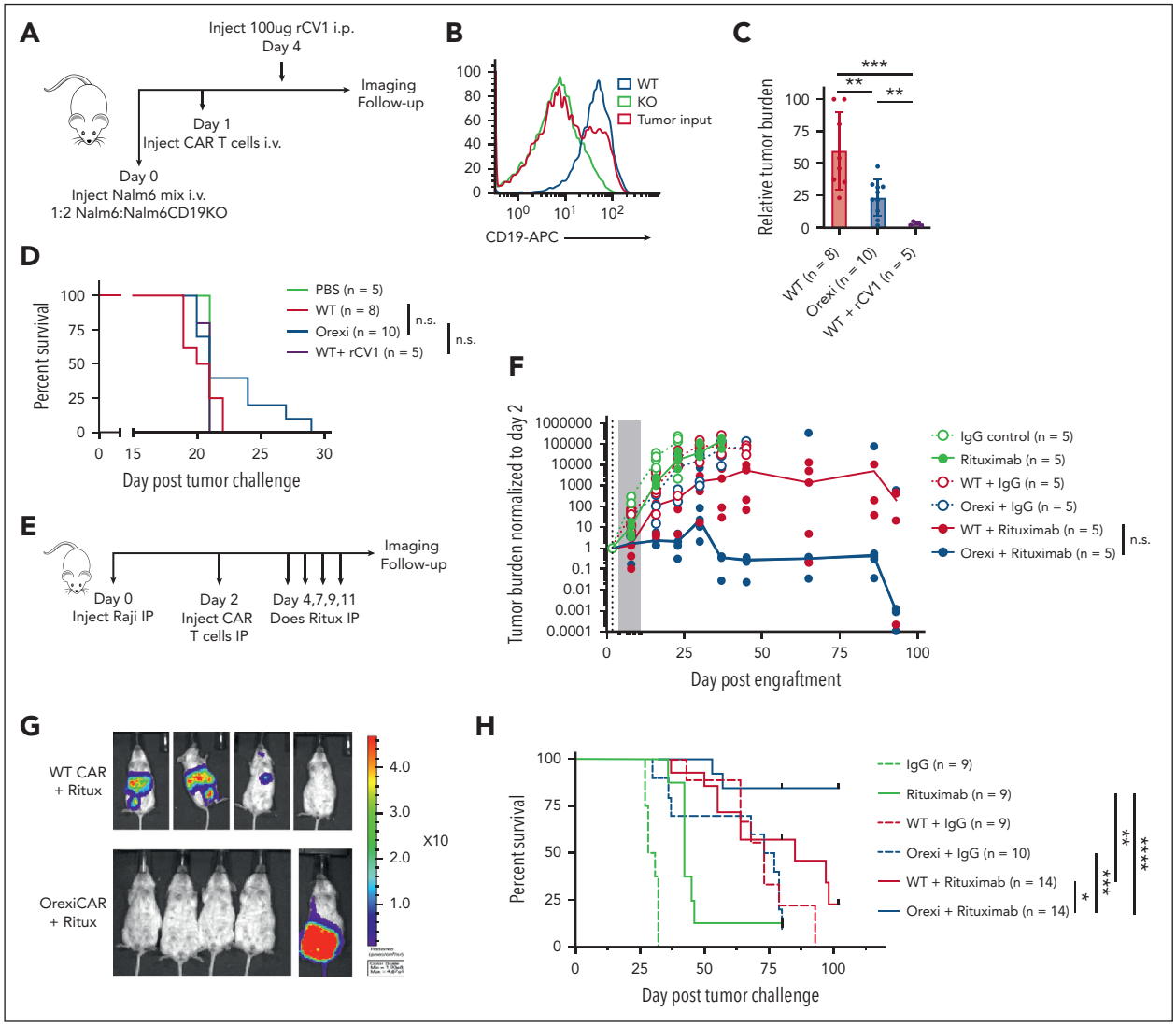

Figure 4. OrexiCAR T cells potentiate the antitumor efficacy of rituximab. (A) NSG mice that received engraftment with a 1:2 ratio of Nalm6-GFP/Luc and Nalm6-CD19KO-GFP/Luc were treated with WT or OrexiCAR T cells. (B) Loss of CD19 expression in Nalm6 KO was confirmed via flow cytometry. (C) Tumor burden at day 9 after engraftment was quantified using BLI and normalized to highest tumor burden. Combined 2 independent experiments. (D) Survival curves for treated mice from 2 independent experiments. (E) NSG mice that underwent engraftment with Raji-GFP/Luc tumor cells IP were treated with 5e5 WT or OrexiCAR T cells and subsequently treated with rituximab or control antibody. (F) Tumor burden was measured over time using BLI (median tumor burden line is drawn) and shown for day 86 after engraftment in (G). (H) Combined survival curves for treated mice from 2 to 3 independent experiments. Statistics were performed using Student *t* test or log-rank survival analysis.

translated to a markedly increased overall survival among animals treated with OrexiCAR T cells and rituximab (Figure 4H). In addition, OrexiCAR T cells plus rituximab significantly improved the median overall survival (86 days) compared with WT CAR T cells in combination with soluble rCV1 and rituximab (59 days) or CV1 plus rituximab (47 days) (supplemental Figure 9). These results in 3 models demonstrate the additive benefits of CAR T cells and mAb therapy, which are further potentiated by OrexiCAR-CV1 secretion.

Enhanced effects of CD19 CAR T cells plus rituximab are due to improved ADCP activity

Next, we sought to understand the mechanisms at play between CAR T cells and mAb therapy. As T cells can express Fc receptors after activation, we questioned whether the presence of the mAb might improve overall T-cell activation and cytotoxicity.[33,34] We found no significant difference in CAR-specific lysis in vitro when rituximab was added to the T-cell and tumor cell coculture after 48 hours (supplemental Figure 10A), suggesting that rituximab did not improve CAR T-cell–mediated lysis.

Next, we questioned whether CAR T cells expand or persist differently in vivo when combined with a tumor-targeted mAb vs without the mAb. CAR T cells that also expressed a *Gaussia* luciferase reporter gene, were tracked in vivo using BLI.[35] We found there was no difference in the expansion or persistence of the CAR T cells in the presence of a tumor-specific mAb, with peak expansion at 48 hours; by 120 hours, cells were not detectable and were not distinguishable from the background (supplemental Figure 10B).

In contrast, the treatment of mice with clodronate to reduce macrophages abrogated the therapeutic effect of rituximab in NSG mice (supplemental Figure 10C), indicating the antitumor effect was largely mediated by mAb-directed ADCP. Therefore, we hypothesized that CAR T cells may enhance mAb efficacy via secreted cytokines and proteins after activation. To test this, we used control CAR T cells (4HCART) targeted to an off-target tumor antigen (MUC16) and treated NSG mice engrafted with Raji tumors IP. Interestingly, 4HCART cells combined with rituximab reduced tumor burden to the same extent as CD19-targeted CAR T cells (supplemental Figure 10D-E). The 4HCAR T cells had no antitumor effect when given with control mAb. This suggested that the CAR T-cell–specific cytolysis plays a minimal role in the mechanism of enhancing mAb activity when given in combination and that CAR T cells alone could enhance ADCP or ADCC, which is then further potentiated by CD47 blockade by use of OrexiCARs.

To exclude the possibility of xenoreactive T cells causing the antitumor effects, we cocultured CD19 CAR T cells in vitro with target cells (Raji) for 2 days in serum-free media. We then removed the cells and injected the supernatant fluid into tumor-bearing mice beginning on day 2 and then dosed on the same days as mAb treatment (supplemental Figure 10F). PCM enhanced the survival of rituximab-treated mice but not of mice that received the control antibody (supplemental Figure 10G). Although T-cell subpopulations can sometimes express Fc receptors that are typically of low-affinity classes and exhibit weak ADCC, these data (supplemental Figure 10F-G) suggest that the engagement of the mAb with the T cell is not a dominant mechanism for the improved cytolytic activity. Therefore, we concluded that CAR T cells improved specific mAb-mediated activity via secreted cytokines.

OrexiCAR T cells overcome immunosuppression of M2s

To explore the mechanisms of improved antitumor activity by OrexiCARs, we tested how CAR T cells behave in the presence of immunosuppressive cells in vitro. To do so, we used tumor-promoting M2s, which have been shown to dampen immune responses within the TME of several cancers (supplemental Figure 11).[36-40] We differentiated primary $CD14^+$ monocytes into M2s using a previously described protocol.[27] Using autologous T cells, we generated $CD19^-$targeted WT and OrexiCAR T cells and cocultured them with M2s and tumor cells and confirmed M2s that showed reduced antitumor activity (Figure 5A; supplemental Figures 12 and 13). After 4 and 24 hours, OrexiCAR T cells showed greater tumor cell lysis over WT CAR T cells (Figure 5B). Without M2s, WT CAR T cells killed tumor cells in comparison with OrexiCAR T cells, but WT CAR T cells were greatly suppressed when cultured with M2s (Figure 5C).

To elucidate the role of M2s in observed tumor lysis, polarized macrophages were cultured with Raji tumor cells, in either WT or OrexiCAR T-cell supernatant (supplemental Figure 11). The supernatant harvested from OrexiCAR T cells improved macrophage-mediated tumor lysis, which is further potentiated upon addition of rituximab (Figure 5D). To probe the mechanism of the observed changes in macrophage polarization after coculture with OrexiCAR T cells or their supernatant, we then analyzed the secreted cytokine profile using Luminex technology. Cocultures containing WT CAR T cells or their supernatant contained higher levels of IL-10 (Figure 5E), indicating an immunosuppressive environment. Analogously, cocultures containing OrexiCAR T cells or their supernatants had significantly higher levels of interferon gamma (IFN-γ) (Figure 5F). Because of the reduction of IL-10 and increase in IFN-γ levels, the data suggest that OrexiCARs reversed the functional immunosuppression of M2s and enabled greater immune activation and tumor lysis.

To test whether the improved tumor lysis by macrophages was due to CV1 secretion, we cocultured M2s alone with Raji tumor cells in OrexiCAR supernatant or WT CAR supernatant supplemented with rCV1. The addition of rCV1 was sufficient to promote tumor lysis by macrophages, a reversal of the previously observed immunosuppression (Figure 5G). When WT CAR T cells were cocultured with M2s and tumor cells in OrexiCAR supernatant, tumor lysis was restored, which was mimicked in the addition of rCV1 to WT supernatant (Figure 5H).

To understand which mechanism is likely responsible for the enhanced OrexiCAR efficacy we observed in Figure 4F,H, we investigated the repolarization of NSG macrophages in vivo using the same mouse model (supplemental Figure 14A). We showed there is no difference in the number of macrophages in intraperitoneal lavage samples as measured by F4/80, but OrexiCAR-treated mice show increased amounts of CD80 and CD86, known markers of mouse M1s,[41] on these macrophages (supplemental Figure 14B-D).

Finally, we also investigated the in vivo efficacy of OrexiCARs in NSG mice using a subcutaneous mixed tumor model of Raji and human M2s (supplemental Figure 15A). Tumor burden as measured by calipers showed reduced tumor burden in the OrexiCAR arm (supplemental Figure 15B). In addition, OrexiCAR-treated mice had a median survival benefit of 20 days and a tail of survival now ongoing at 100 days when compared with WT CAR-bearing mice (supplemental Figure 15C). Taken together, these data demonstrate the ability of OrexiCAR T cells to ameliorate immunosuppression by phagocytes, likely via secreted CV1, which was probably responsible for the improved antitumor activity.

Primary murine T cells can be engineered to secrete CV1

To test whether OrexiCAR T cells could reverse immunosuppression in vivo, we adapted the OrexiCAR system to be tested in an immune-competent mouse model. In these experiments, we used PMEL transgenic T cells, which target GP100 peptide major histocompatibility complex (MHC) on B16F10 melanoma cells. To generate Orexi-PMEL T cells (CV1-PMEL), PMEL T cells were transduced with a vector encoding CV1 and GFP (supplemental Figure 16A-B) or a control vector (mock). CV1 secretion was confirmed using ELISA (supplemental Figure 16C). There was no difference in tumor cell killing between the mock-transduced and CV1-transduced PMEL T cells (supplemental Figure 16D). Importantly, CV1 binds to and blocks mouse CD47 but with a far lower affinity compared to

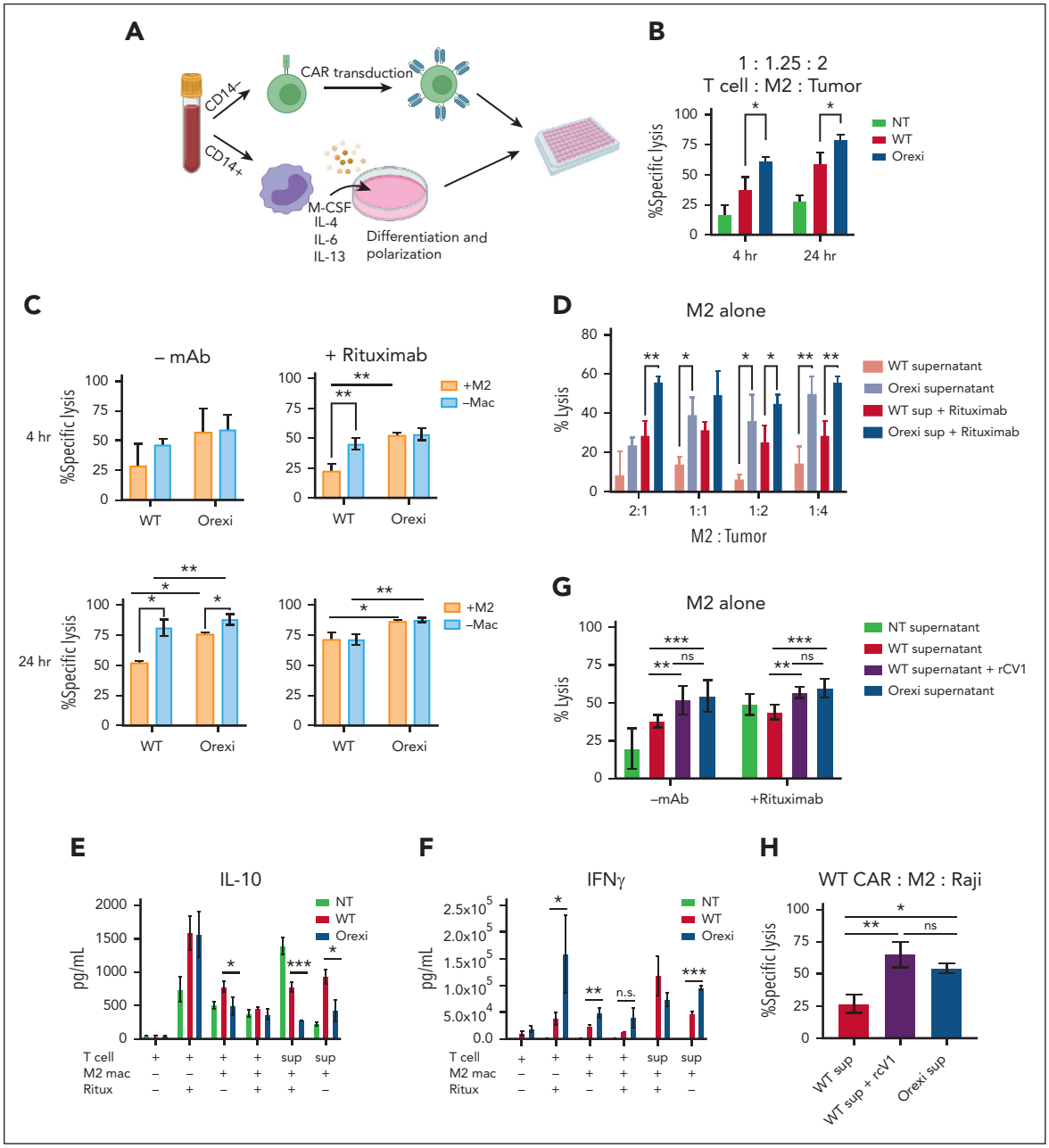

Figure 5. OrexiCAR T cells overcome M2-mediated immunosuppression. (A) Schematic of experimental set up. (B) T cells, M2s, and Raji-GFP/Luc tumor cells were cocultured for 4 and 24 hours. Tumor lysis was measured using luminescence. (C) Same experiment in panel B, which compared effect of M2s on T-cell–mediatedtumor lysis. (D) M2s alone were cultured with Raji tumor cells at indicated ratios in either WT or OrexiCAR supernatant ± rituximab (1μg/mL). (E-F) Supernatants from the indicated experiments were harvested after 24 hours and analyzed using Luminex for IL-10 (E) and IFN-γ (F). (G) M2s alone were cultured with Raji tumor cells in WT supernatant, WT supernatant supplemented with recombinant CV1 in excess, or OrexiCAR supernatant for 4 hours, and tumor lysis was measured. (H) WT CAR T cells, M2s, and Raji tumor cells were cocultured for 4 hours in the indicated supernatant. Data shown are from 1 representative human donor; all experiments were corroborated with 2 or more donors. Statistics were performed using student *t* test. –mac, no macrophages present; mac, macrophage; NT, nontransduced T cells; ritux, rituximab; sup, supernatant harvested from transduced T cells.

human CD47.[17,42] These data recapitulated the results observed in the human OrexiCAR system described earlier.

CV1-PMEL T cells reprogram the TME in vivo

To assess the impact of CV1-secreting PMEL T cells on the TME, immune-competent mice engrafted with B16F10 subcutaneously were treated with mock- or CV1-transduced PMEL T cells. Five days after T-cell injection, tumors were harvested and analyzed (Figure 6A). Firstly, we found that tumor-infiltrating DCs (Figure 6B-D), but not macrophages (Figure 6C-D; supplemental Figure 16E), showed increased MHCII expression after treatment with CV1-PMEL T cells compared with those with mock-transduced PMELs. Interestingly, CV1-PMEL–treated mice had a higher percentage of $CD11b^{+}$–infiltrating $CD45^{+}$ cells than $CD11c^{+}$ (Figure 6E,F). This indicated that a higher proportion of tumor-infiltrating cells were macrophages and not

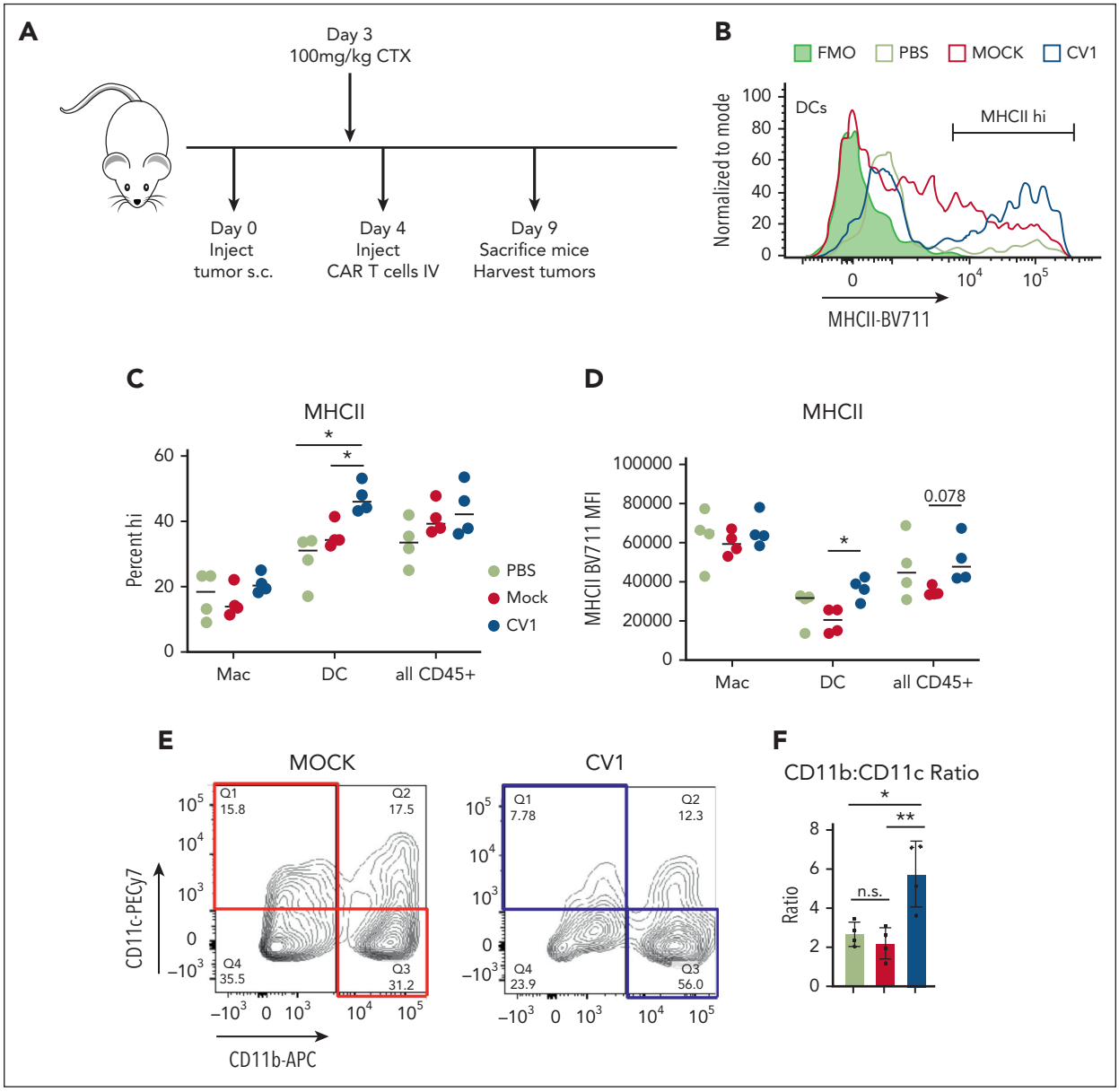

Figure 6. Orexi T cells reprogram the TMEs in immune-competent hosts. (A) C57/BL6 mice underwent engraftment subcutaneously with 2e6 B16F10 tumor cells and, after 4 days, were treated with PBS, mock-transduced, or CV1-transduced PMEL T cells. (B) Tumors were harvested and analyzed for MHCII expression, shown for representative histograms, and quantified in (C) and (D). (E) $CD45^+$ cells from harvested B16 tumors were gated for CD11b vs CD11c expression, representative contour plot shown with quantifications in (F). Statistics were performed using student *t* test. FMO, fluorescence minus one; PBS, phosphate-buffered saline.

DCs. This was further confirmed by an increased $F4/80^+$ population of CV1-PMEL–treated mice (supplemental Figure 16F). This was interesting for 2 reasons: (1) although CV1-PMEL T-cell–treated mice had a lower proportion of DCs than those with mock PMEL-treated tumors, these DCs that were present were more activated, using MHCII expression as a surrogate and (2) CD11b agonism was previously shown to promote immune-stimulatory TMEs in a variety of tumor types.[38,43,44] Given the observed increase in $CD11b^+$ cells, we hypothesized that CV1 secretion in the tumor may be priming macrophages toward an activated phenotype, even though canonical activation markers were not changed. Collectively, these data indicate that Orexi-treatment (CV1-PMEL) causes TME reprogramming, leading to activated DCs and primed macrophages.

T-cell–secreted CV1 evades the systemic CD47 antigen sink

We demonstrated that human OrexiCARs secreted low but detectable levels of CV1 that bound to peripheral blood in an immunodeficient model (Figure 2F). Thus, to validate our findings about the xenograft, we questioned whether OrexiCARs circumvent the antigen sink in an immune-competent, syngeneic model. Mice were pretreated with cyclophosphamide and then injected IV with CV1 or GFP (mock-transduced control) PMEL T cells and B16F10 tumor cells at an effector to target ratio of 4:1. Tumor cells were added to expand the transferred PMEL T cells. Mice receiving GFP-PMEL T cells were also dosed with either a single dose or a daily dose of soluble rCV1 (supplemental Figure 17A). Harvested peripheral blood showed no detectable CV1 from

CV1-PMEL–treated mice (CV1-T), whereas systemically administered soluble rCV1 uniformly coated blood cells (GFP-T + rCV1; supplemental Figure 17B). This led to a reduction in detectable CD47 on peripheral blood cells only in mice receiving rCV1 and not CV1-PMEL T cells (supplemental Figure 17C). As expected, daily dosing of rCV1 steadily blocked CD47 (supplemental Figure 17E) with consistent levels of CV1 bound to peripheral blood (supplemental Figure 17F), whereas levels of CD47 blocking and CV1 tapered off for 72 hours after only a single dose. Strikingly, OrexiCAR-PMEL–treated mice never had detectable levels of CV1 in the blood up to 7 days after T-cell injection (supplemental Figure 17F). Altogether, these data show that T cells can be engineered to specifically deliver CV1 to tumors, avoiding the systemic CD47 antigen sink.

Discussion

CAR T cells are limited by pharmacologic, immunologic, and biologic hurdles, resulting in tumor regrowth and disease relapse.[2,45] Here, we demonstrated that CAR T cells augmented an orthogonal mAb to better eradicate lymphomas and antigen-heterogeneous tumors. Although most patients receiving CD19 CAR T cells are refractory to rituximab, reinvigoration of innate immune cells may reverse this effect, allowing for effective redosing of the mAb, which we demonstrated in a rituximab-refractory tumor model. These results may have immediate clinical relevance because the cells and antibodies used here (CD19 CAR T cells and rituximab) are both Food and Drug Administration–approved agents used widely in various B-cell neoplasms. To further enhance the ability of the CAR T cells to potentiate mAb therapy, we engineered OrexiCAR T cells, which secrete a potent CD47-SIRPα pathway blocker, CV1. In addition, the OrexiCAR system can be easily adapted to target other tumor-associated antigens.

To understand the potential mechanisms of OrexiCARs on the TME, we generated autologous M2s (suppressive) to coculture with OrexiCAR and WT CAR T cells. We demonstrated that OrexiCAR T cells, but not WT CAR T cells, functioned better in the presence of M2s, enhanced macrophage ADCC/ADCP in vitro and in vivo, shifted the macrophage phenotype away from an immunosuppressive M2 phenotype, and demonstrated enhanced antitumor effects in vivo. Given that most of these experiments were performed using NSG mice, which lack B, T, and natural killer cells, we conclude that macrophages specifically contributed to the therapeutic benefit observed; however, direct ADCC activity by neutrophils cannot be ruled out in our system.[46] Therefore, we postulated that OrexiCAR T cells could overcome and reverse immunosuppression by M2s, which can define the TME in a variety of cancers.[47-49]

Finally, to validate our in vitro results, we engineered murine CV1-PMEL T cells and demonstrated improved innate immune cell activation within the TME of immune-competent hosts.

Both preclinical and clinical studies have suggested CD47 blockade is a promising immunotherapeutic approach to cancer.[17,23,25,28,29] However, the ubiquitous expression of CD47 provides an enormous receptor sink, therefore requiring frequent large doses. In addition, ubiquitous cell-surface expression of CD47 can result in human clinical toxicities.[17,50,51] Our strategy, using OrexiCAR T cells, is able to bypass the receptor sink through local delivery (as has been observed with IL-12 CAR T cells).[9,52] We additionally found that CV1 secreted by PMEL T cells does not saturate the antigen sink.

Accordingly, we focused our studies on NSG mice,[53-55] which bind to human CD47 and allow for the engraftment of human tumor cells capable of shutting down endogenous mouse effectors (macrophages). In these models, we were able to demonstrate TME reprogramming by Orexi T cells in vivo.

CAR T cells secreting single-domain antibody fragments (VHHs) against CD47 have recently been reported.[52] This approach[52] as well as ours, described here, use CD47 blockers that are small in protein size, allowing room for modularity on the CAR vectors. An advantage to our approach is the use of CV1, a high-affinity protein with a short plasma half-life. The prolonged serum half-life of VHHs can be helpful in systemic therapy but may cause toxicities from increased VHH diffusion to off-target organs. Furthermore, CV1 binds both mouse and human CD47, allowing for the study of both syngeneic and human xenograft systems, whereas the mechanisms and outcomes described using a fully syngeneic VHH in a mouse system are not easily translated for human use. In addition, we used CARs and antibodies that are already approved agents. Furthermore, here we were able to achieve durable remissions and tumor cures in a highly aggressive lymphoma model, bolstering the clinical potential. Finally, we characterized a mechanism that may account for the improved OrexiCAR T-cell efficacy through the creation of a more immune-stimulating microenvironment.

The work presented here demonstrates the use of CAR T cells not only as a direct antitumor agent but also a targeted cellular micropharmacy to activate innate immune effectors. Furthermore, the addition of CV1 to current CAR T-cell constructs may act as an adjuvant, thereby mitigating tumor escape by loss of CAR T-cell antigens. Altogether, to our knowledge, this strategy represents a novel platform that may improve clinical outcomes in hematopoietic cancers treated with CAR T cells.

Acknowledgments

The authors thank Aaron Chang for generating the Nalm6-CD19KO cells and Renier Brentjens, Dinali Wijewarnasuriya, and Jonathan F. Khan, Memorial Sloan Kettering Cancer Center (MSKCC), for helpful discussions and reagents. The authors also thank the K. C. Garcia lab at Stanford University for the soluble CV1 provided for in vitro and sink experiments. The authors also acknowledge Richard O'Reilly and Marcel Van den Brink (MSKCC) for their thoughtful discussions.

This work was supported by National Institutes of Health (NIH), National Cancer Institute (NCI) grants F31 CA239511 (M.M.D.), from F31 CA254331 to 01 (C.M.B.), F32 CA224438 (T.J.G.), NIH, National Institute of General Medical Sciences grants T32 GM115327 and T32 GM136640 (K.C.V), NIH grants P30008748, P01 23766, and R01 55349 (D.A.S.), NIH, NCI grant R35 CA241894 (D.A.S.), and by Experimental Therapeutics Center at MSKCC (D.A.S.), Greenburg Trust Fund (D.A.S.), Lymphoma SPORE (D.A.S.), and the Emerson Collective (D.A.S.).

Authorship

Contribution: D.A.S. and A.Y. conceptualized the work; M.M.D. and K.G.K. designed the study; M.M.D., C.M.B., K.G.K., P.W., S.K., S.A.P., and T.J.G. performed the methodology; M.M.D., C.M.B., K.G.K., P.W., S.K., S.P., and N.A. performed investigation; M.M.D., K.G.K., and D.A.S

analyzed the data and wrote the manuscript; and K.G.K., M.M.D., D.A.S., C.M.B., and K.C.V. edited and finalized the manuscript.

Conflict-of-interest disclosure: D.A.S. has equity in or is a consultant for Actinium Pharmaceuticals, Arvinas, Eureka Therapeutics, Iovance Biotherapeutics, OncoPep, CoImmune, and Pfizer. MSKCC has filed for patent protection behalf of M.M.D., T.J.G., and D.A.S. for the inventions described in this article. T.J.G. is currently employed by ArsenalBio. A.Y. is currently employed by AstraZeneca. The remaining authors declare no competing financial interests.

ORCID profiles: M.M.D., 0000-0003-1731-1502; K.G.K., 0000-0002-0988-1508; P.W., 0000-0002-1850-4253; S.A.P., 0000-0002-2950-278X; S.K., 0000-0002-9197-9167; C.M.B., 0000-0001-9290-4223.

Correspondence: David A. Scheinberg, Memorial Sloan Kettering Cancer Center, 1275 York Ave, New York, NY 10065; email: scheinbd@mskcc.org.

Footnotes

Submitted 15 March 2022; accepted 16 January 2023; prepublished online on *Blood* First Edition 25 January 2023. https://doi.org/10.1182/blood.2022016101.

*M.M.D. and K.G.K. contributed equally to this work.

Data are available on request from the corresponding author, David A. Scheinberg (scheinbd@mskcc.org).

The online version of this article contains a data supplement.

There is a *Blood* Commentary on this article in this issue.

The publication costs of this article were defrayed in part by page charge payment. Therefore, and solely to indicate this fact, this article is hereby marked "advertisement" in accordance with 18 USC section 1734.

REFERENCES

1. Sadelain M, Rivière I, Riddell S. Therapeutic T cell engineering. *Nature*. 2017;545(7655):423-431.
2. Majzner RG, Mackall CL. Tumor antigen escape from CAR T-cell therapy. *Cancer Discov*. 2018;8(10):1219-1226.
3. Chong EA, Ruella M, Schuster SJ; Lymphoma Program Investigators at the University of Pennsylvania. Five-year outcomes for refractory B-Cell lymphomas with CAR T-cell therapy. *N Engl J Med*. 2021;384(7):673-674.
4. Gardner TJ, Bourne CM, Dacek MM, et al. Targeted Cellular Micropharmacies: Cells Engineered for Localized Drug Delivery. *Cancers (Basel)*. 2020;12(8):2175.
5. Rafiq S, Yeku OO, Jackson HJ, et al. Targeted delivery of a PD-1-blocking scFv by CAR-T cells enhances anti-tumor efficacy in vivo. *Nat Biotechnol*. 2018;36(9):847-856.
6. Pegram HJ, Lee JC, Hayman EG, et al. Tumor-targeted T cells modified to secrete IL-12 eradicate systemic tumors without need for prior conditioning. *Blood*. 2012;119(18):4133-4141.
7. Hu B, Ren J, Luo Y, et al. CAR T cells secreting IL18 augment antitumor immunity and increase T cell proliferation and costimulation. *Cell Rep*. 2017;20(13):3025-3033.
8. Koneru M, Purdon TJ, Spriggs D, Koneru S, Brentjens RJ. IL-12 secreting tumor-targeted chimeric antigen receptor T cells eradicate ovarian tumors in vivo. *OncoImmunology*. 2015;4(3):e994446.
9. Yeku OO, Purdon TJ, Koneru M, Spriggs D, Brentjens RJ. Armored CAR T cells enhance antitumor efficacy and overcome the tumor microenvironment. *Sci Rep*. 2017;7(1):10541.
10. Liu E, Tong Y, Dotti G, et al. Cord blood NK cells engineered to express IL-15 and a CD19-targeted CAR show long-term persistence and potent antitumor activity. *Leukemia*. 2018;32(2):520-531.
11. Kuhn NF, Purdon TJ, van Leeuwen DG, et al. CD40 ligand-modified chimeric antigen receptor T cells enhance antitumor function by eliciting an endogenous antitumor response. *Cancer Cell*. 2019;35(3):473-488.e6.
12. Zhao Z, Condomines M, van der Stegen SJC, et al. Structural design of engineered costimulation determines tumor rejection kinetics and persistence of CAR T cells. *Cancer Cell*. 2015;28(4):415-428.
13. Giavridis T, van der Stegen SJC, Eyquem J, Hamieh M, Piersigilli A, Sadelain M. CAR T cell-induced cytokine release syndrome is mediated by macrophages and abated by IL-1 blockade letter. *Nat Med*. 2018;24(6):731-738.
14. Norelli M, Camisa B, Barbiera G, et al. Monocyte-derived IL-1 and IL-6 are differentially required for cytokine-release syndrome and neurotoxicity due to CAR T cells. *Nat Med*. 2018;24(6):739-748.
15. Teachey DT, Lacey SF, Shaw PA, et al. Identification of predictive biomarkers for cytokine release syndrome after chimeric antigen receptor T-cell therapy for acute lymphoblastic leukemia. *Cancer Discov*. 2016;6(6):664-679.
16. Santomasso B, Bachier C, Westin J, Rezvani K, Shpall EJ. The other side of CAR T-cell therapy: cytokine release syndrome, neurologic toxicity, and financial burden. *Am Soc Clin Oncol Educ B*. 2019;39:433-444.
17. Weiskopf K, Ring AM, Ho CCM, et al. Engineered SIRPα variants as immunotherapeutic adjuvants to anti-cancer antibodies. *Science*. 2013;341(6141):88-91.
18. Mathias MD, Sockolosky JT, Chang AY, et al. CD47 blockade enhances therapeutic activity of TCR mimic antibodies to ultra low density cancer epitopes. *Leukemia*. 2017;31(10):2254-2257.
19. Li Y, Lu S, Xu Y, et al. Overexpression of CD47 predicts poor prognosis and promotes cancer cell invasion in high-grade serous ovarian carcinoma. *Am J Transl Res*. 2017;9(6):2901-2910.
20. Matlung HL, Szilagyi K, Barclay NA, van den Berg TK. The CD47-SIRPα signaling axis as an innate immune checkpoint in cancer. *Immunol Rev*. 2017;276(1):145-164.
21. Chao MP, Weissman IL, Majeti R. The CD47-SIRP pathway in cancer immune evasion and potential therapeutic implications. *Curr Opin Immunol*. 2012;24(2):225-232.
22. Chao MP, Alizadeh AA, Tang C, et al. Anti-CD47 antibody synergizes with rituximab to promote phagocytosis and eradicate non-Hodgkin lymphoma. *Cell*. 2010;142(5):699-713.
23. Liu X, Pu Y, Cron K, et al. CD47 blockade triggers T cell–mediated destruction of immunogenic tumors. *Nat Med*. 2015;21(10):1209-1215.
24. Xu MM, Pu Y, Han D, et al. Dendritic cells but not macrophages sense tumor mitochondrial DNA for cross-priming through signal regulatory protein α signaling. *Immunity*. 2017;47(2):363-373.e5.
25. Weiskopf K, Jahchan NS, Schnorr PJ, et al. CD47-blocking immunotherapies stimulate macrophage-mediated destruction of small-cell lung cancer. *J Clin Invest*. 2016;126(7):2610-2620.
26. Sockolosky JT, Dougan M, Ingram JR, et al. Durable antitumor responses to CD47 blockade require adaptive immune stimulation. *Proc Natl Acad Sci U S A*. 2016;113(19):E2646-E2654.
27. Zarif JC, Hernandez JR, Verdone JE, Campbell SP, Drake CG, Pienta KJ. A phased strategy to differentiate human CD14+ monocytes into classically and alternatively activated macrophages and dendritic cells. *Biotechniques*. 2016;61(1):33-41.
28. Advani R, Flinn I, Popplewell L, et al. CD47 blockade by Hu5F9-G4 and rituximab in non-Hodgkin's lymphoma. *N Engl J Med*. 2018;379(18):1711-1721.
29. Sikic BI, Lakhani N, Patnaik A, et al. First-in-human, first-in-class phase i trial of the anti-CD47 antibody Hu5F9-G4 in patients with advanced cancers. *J Clin Oncol*. 2019;37(12):946-953.
30. Leclair P, Liu C, Monajemi M, Reid GS, Sly LM, Lim CJ. CD47-ligation induced cell death in T-acute lymphoblastic leukemia article. *Cell Death Dis*. 2018;9(544):1-14.

31. Mateo V, Lagneaux L, Bron D, et al. CD47 ligation induces caspase-independent cell death in chronic lymphocytic leukemia. *Nat Med*. 1999;5(11):1277-1284.

32. Pettersen RD, Hestdal K, Olafsen MK, Lie SO, Lindberg FP. CD47 signals T cell death. *J Immunol*. 1999;162(12):7031-7040.

33. Chauhan AK. Human CD4+ T-cells: a role for low-affinity Fc receptors. *Front Immunol*. 2016;7(215):215.

34. Dhanji S, Tse K, Teh H-S. The low affinity Fc receptor for IgG functions as an effective cytolytic receptor for self-specific CD8 T cells. *J Immunol*. 2005;174(3):1253-1258.

35. Santos EB, Yeh R, Lee J, et al. Sensitive in vivo imaging of T cells using a membrane-bound Gaussia princeps luciferase. *Nat Med*. 2009; 15(3):338-344.

36. Jiménez I, Carabia J, Bobillo S, et al. Repolarization of tumor infiltrating macrophages and increased survival in mouse primary CNS lymphomas after XPO1 and BTK inhibition. *J Neuro Oncol*. 2020; 149(1):13-25.

37. Zhang Y, Xiang J, Sheng X, et al. GM-CSF enhanced the effect of CHOP and R-CHOP on inhibiting diffuse large B-cell lymphoma progression via influencing the macrophage polarization. *Cancer Cell Int*. 2021;21:141.

38. Geraghty T, Rajagopalan A, Aslam R, et al. Positive allosteric modulation of CD11b as a novel therapeutic strategy against lung cancer. *Front Oncol*. 2020;10:748.

39. Werner L, Dreyer JH, Hartmann D, et al. Tumor-associated macrophages in classical Hodgkin lymphoma: hormetic relationship to outcome. *Sci Rep*. 2020;10(1):9410-9411.

40. Abdulla OA, Nagarkatti PS, Nagarkatti M. Regulation of macrophages in tumor microenvironment by microRNA in T cell lymphoma-bearing mice. *J Immunol*. 2020; 204(1_Supplement):164.18.

41. Mantovani A, Sica A, Sozzani S, Allavena P, Vecchi A, Locati M. The chemokine system in diverse forms of macrophage activation and polarization. *Trends Immunol*. 2004;25(12): 677-686.

42. Kauder SE, Kuo TC, Harrabi O, et al. ALX148 blocks CD47 and enhances innate and adaptive antitumor immunity with a favorable safety profile. *PLoS One*. 2018;13(8):e0201832.

43. Schmid MC, Khan SQ, Kaneda MM, et al. Integrin CD11b activation drives anti-tumor innate immunity. *Nat Commun*. 2018;9: 5379.

44. Panni RZ, Herndon JM, Zuo C, et al. Agonism of CD11b reprograms innate immunity to sensitize pancreatic cancer to immunotherapies. *Sci Transl Med*. 2019;11(499):eaau9240.

45. Grant M, Bollard CM. Developing T-cell therapies for lymphoma without receptor engineering. *Blood Adv*. 2017;1(26):2579-2590.

46. Behrens LM, van den Berg TK, van Egmond M. Targeting the CD47-SIRPα Innate Immune Checkpoint to Potentiate Antibody Therapy in Cancer by Neutrophils. *Cancers*. 2022;14:3366.

47. Xu ZZ, Xu S, Kuhlmann A, Kaech SM. The role of CD36 in macrophage lipid metabolism and function in tumor microenvironment. *J Immunol*. 2020; 204(suppl 1):240.9.

48. Ruella M, Klichinsky M, Kenderian SS, et al. Overcoming the immunosuppressive tumor microenvironment of Hodgkin lymphoma using chimeric antigen receptor T cells. *Cancer Discov*. 2017;7(10):1154-1167.

49. Qiu SQ, Waaijer SJH, Zwager MC, de Vries EGE, van der Vegt B, Schroder CP. Tumor-associated macrophages in breast cancer: innocent bystander or important player? *Cancer Treat Rev*. 2018;70:178-189.

50. Ingram JR, Blomberg OS, Sockolosky JT, et al. Localized CD47 blockade enhances immunotherapy for murine melanoma. *Proc Natl Acad Sci U S A*. 2017;114(38): 10184-10189.

51. Veillette A, Chen J. CD47 immune checkpoint blockade in anticancer therapy. *Trends Immunol*. 2018;39(3):173-184.

52. Xie YJ, Dougan M, Ingram JR, et al. Improved anti-tumor efficacy of chimeric antigen receptor T cells that secrete single-domain antibody fragments. *Cancer Immunol Res*. 2020;8(4):518-529.

53. Kwong LS, Brown MH, Barclay AN, Hatherley D. Signal-regulatory protein α from the NOD mouse binds human CD47 with an exceptionally high affinity– implications for engraftment of human cells. *Immunology*. 2014;143(1):61-67.

54. Yamauchi T, Takenaka K, Urata S, et al. Polymorphic Sirpa is the genetic determinant for NOD-based mouse lines to achieve efficient human cell engraftment. *Blood*. 2013;121(8):1316-1325.

55. Subramanian S, Parthasarathy R, Sen S, Boder ET, Discher DE. Species- and cell type-specific interactions between CD47 and human SIRPalpha. *Blood*. 2006;107(6): 2548-2556.